

Coupled-Channels Calculation of the Elastic and Inelastic Scattering of Protons by Carbon-12

A. C. L. BARNARD

IBM Scientific Center, Houston, Texas

(Received 14 November 1966)

The elastic scattering of protons by C^{12} exhibits the following resonances with an appreciable fraction of the single-particle width: $E_p=0.461$ MeV ($s_{1/2}$), 1.748 MeV ($d_{5/2}$), and ≈ 6.7 MeV ($d_{3/2}$). A narrow $d_{5/2}$ resonance is observed at 4.808 MeV and an anomaly in the $d_{3/2}$ phase shift at ≈ 5.3 MeV. It is demonstrated by means of a coupled-channel calculation that these last two features are due to the resonance in the inelastic channel (C^{12}^*+p) corresponding to the 0.461-MeV s -wave resonance in the elastic channel. The experimental s - and d -wave phase shifts and damping parameters are accurately reproduced after adjustment of the depth of square-well potentials. The coupled-channel calculation also demonstrates that a resonance may be switched from one channel to another by changing the strength of the coupling.

I. INTRODUCTION

THE scattering of protons by C^{12} has been carefully studied up to a proton energy $E_p \approx 9$ MeV.¹⁻⁶ Below $E_p=4.800$ MeV only elastic scattering is possible, and the collision matrix diagonal element has the form $e^{2i\delta}$, so that the real phase shifts δ for the partial waves completely specify the scattering. Above this energy both elastic and inelastic scattering are possible and the matrix element may be written $\alpha e^{2i\delta}$, where $\alpha < 1$. Thus two real quantities, the phase shift δ and the "damping parameter" α , for each partial wave may be used to describe the processes.

The $s_{1/2}$ phase shift is experimentally observed to pass through a resonance at $E_p=0.461$ MeV (Fig. 1). Unfortunately, the numerical values of the experimental phase shifts over the resonance were not tabulated in

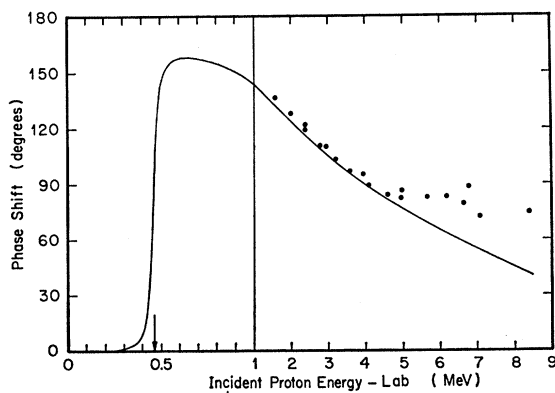


FIG. 1. The s -wave phase shifts for ($C^{12}+p$). The dots are experimental values and the solid curve was calculated as described in the text. Note the expanded energy scale below 1 MeV.

¹ H. L. Jackson and A. I. Galonsky, Phys. Rev. **89**, 370 (1953).

² C. W. Reich, G. C. Phillips, and J. L. Russell, Jr., Phys. Rev. **104**, 143 (1956).

³ S. J. Moss and W. Haeblerli, Nucl. Phys. **72**, 417 (1965).

⁴ A. C. L. Barnard, J. B. Swint, and T. B. Clegg, Nucl. Phys. **86**, 130 (1966).

⁵ A. C. L. Barnard, J. S. Duval, Jr., and J. B. Swint, Phys. Letters **20**, 412 (1966).

⁶ J. S. Duval, Jr., A. C. L. Barnard, J. B. Swint, and T. B. Clegg, Nucl. Phys. (to be published).

the original paper.¹ The points at higher energies on Fig. 1 are experimental values.

As shown by the points on Fig. 2, the $d_{5/2}$ phase shift is experimentally observed to pass through a resonance at $E_p=1.748$ MeV with width $\Gamma=66$ keV,¹ and a further narrow resonance occurs at $E_p=4.808$ MeV ($\Gamma=12$ keV).² The experimentally observed behavior of the $d_{3/2}$ phase shift and damping parameter is shown by the points on Fig. 3. There is a very wide ($\Gamma \approx 1.72$ MeV) resonance at which the phase shift passes through $\pi/2$ at $E_p \approx 6.7$ MeV.^{3,4} The corresponding compound-nuclear state apparently has little or no inelastic-scattering width.³ Further activity of the $d_{3/2}$ phase shift is observed between $E_p \approx 5.2$ and 5.5 MeV, corresponding to a $J^\pi=3/2^+$ compound-nuclear state with large inelastic width.² It can be seen from Fig. 3 that the phase shift does not pass through $\pi/2$ in this anomaly.^{5,6} The behavior of the phase shifts for other partial waves is not relevant to this paper.

The differing behavior of the two neighboring anomalies in the $d_{3/2}$ shift is interesting. In terms of the nuclear scattering amplitude $f_j=i(1-U_{jj})$, where U is the collision matrix, the difference is that the path

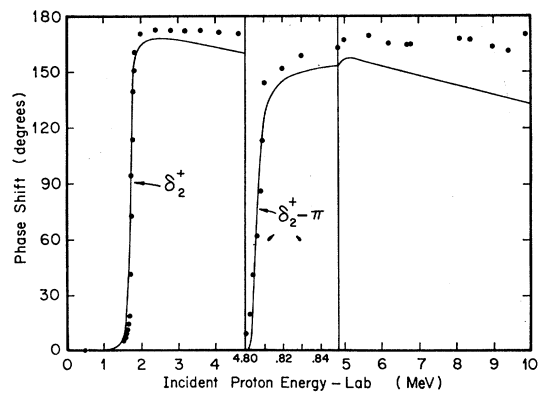


FIG. 2. The dots are experimental values of the $d_{5/2}$ phase shifts for ($C^{12}+p$). Note that the energy scale has been expanded between 4.80 and 4.85 MeV. Above 4.8 MeV, π radians have been subtracted from the phase shifts plotted. The curves were calculated as described in the text.

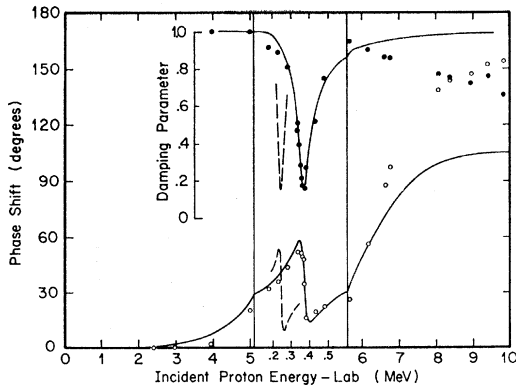


FIG. 3. The open circles are experimental values of the $d_{3/2}$ phase shifts for $(C^{12}+p)$. The dots are the experimental damping parameters. Note that the energy scale has been expanded from $E_p=5.1$ to 5.6 MeV. The solid and dashed curves were calculated as described in the text.

of the amplitude in the complex plane includes or excludes the center of the unitary circle (C on Fig. 4). The points on Fig. 4 show the measured values of the $d_{3/2}$ scattering amplitude as the energy increases over the two anomalies.

The $E_p=0.461$ -MeV resonance in the $s_{1/2}$ phase shift, the $E_p=1.748$ -MeV resonance in the $d_{5/2}$ phase shift and the $E_p\approx 6.7$ -MeV resonance in the $d_{3/2}$ phase shift are of the single-particle type and are qualitatively reproduced by a simple potential scattering calculation. If the nuclear force is represented by a "square-well" potential of radius R , and the Coulomb force neglected in this region, the radial wave functions for $r < R$ are spherical Bessel functions. For $r > R$ the functions are ingoing and outgoing Coulomb waves and the functions

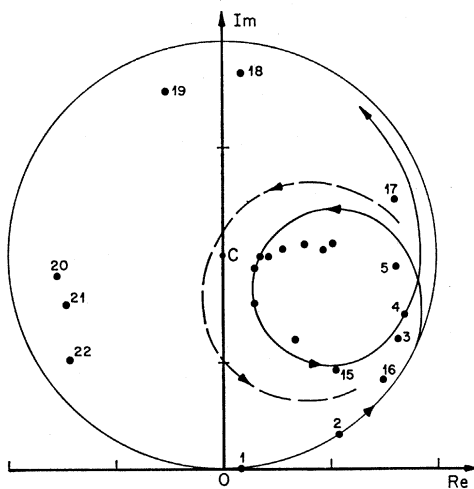


FIG. 4. The $d_{3/2}$ scattering amplitude $f_j=i(1-U_{jj})$ plotted in the complex plane. The points are the experimental values over the 5.3 and 6.7 MeV anomalies, numbered in order of increasing energy. The solid and dashed curves were calculated as described in the text. As the energy is increased the progression is along the curve in the direction of the arrow.

are matched in value and slope at $r=R$. Such a calculation gives resonances wider than those observed experimentally, since the coupling to other channels, both open and closed, is neglected.

Such single-channel calculations completely fail to reproduce the 4.808-MeV $d_{5/2}$ anomaly and the 5.3-MeV $d_{3/2}$ anomaly. It will be shown in this paper that these experimental observations are reproduced by a calculation which includes coupling to the inelastic-scattering channel $(C^{12*}+p)$, which will be called channel 2. The coupling is only included when the channel is open. The threshold for channel 2 is $E_p=4.800$ MeV, assuming $Q=-4.43$ MeV. Since C^{12*} has $J^\pi=2^+$, a $d_{3/2}$ or $d_{5/2}$ compound-nuclear state may decay into $(C^{12*}+p)$ with the l value of the outgoing proton $l_2=0$ or 2, so that two inelastic channels should be considered. However, close to threshold the former is expected to dominate because of its higher penetrability. In the calculations reported in this paper, the maximum number of channels was two (one elastic and one inelastic).

II. GENERAL RESULTS OF COUPLED-CHANNEL CALCULATION

If two channels are considered, the Schrödinger equation may be written

$$\begin{pmatrix} H_{11} & V_{12} \\ V_{21} & H_{22} \end{pmatrix} \begin{pmatrix} \psi_1 \\ \psi_2 \end{pmatrix} = \begin{pmatrix} E_1 & 0 \\ 0 & E_2 \end{pmatrix} \begin{pmatrix} \psi_1 \\ \psi_2 \end{pmatrix}, \quad (1)$$

where V_{12} and V_{21} are the matrix elements which couple the two channels. The process will be considered as scattering of a single particle by a potential well, so that the ψ 's are single-particle wave functions and no antisymmetrization is performed. If the potential is taken to be spherically symmetric, the ψ 's separate in the usual way and the equations for the radial functions u_1 and u_2 are

$$\frac{1}{r^2} \left[\frac{d}{dr} \left(r^2 \frac{d}{dr} \right) - l_1(l_1+1) \right] u_1 + K_{11}^2 u_1 = K_{12}^2 u_2, \quad (2)$$

$$\frac{1}{r^2} \left[\frac{d}{dr} \left(r^2 \frac{d}{dr} \right) - l_2(l_2+1) \right] u_2 + K_{22}^2 u_2 = K_{21}^2 u_1, \quad (3)$$

where

$$K_{ii} = (2m_i/\hbar^2)(E_i - V_{ii}),$$

$$K_{ij} = (2m_j/\hbar^2)V_{ij}.$$

If all three potentials, V_{11} , V_{22} , and V_{12} ($=V_{21}$) are taken to be "square wells" of radius R , and $l_1=l_2$, the solutions for $r < R$ have been given by Tombrello and Phillips⁷:

$$u_1(r) = a_{11} j_l(K_1 r) + a_{22} \left[\frac{K_{22}^2 - K_2^2}{K_{21}^2} \right] j_l(K_2 r), \quad (4)$$

⁷ T. A. Tombrello and G. C. Phillips, Nucl. Phys. **20**, 648 (1960).

$$u_2(r) = a_{11} \left[\frac{K_{11}^2 - K_1^2}{K_{12}^2} \right] j_l(K_1 r) + a_{22} j_l(K_2 r), \quad (5)$$

where

$$K_i^2 = \frac{1}{2}(K_{11}^2 + K_{22}^2) \pm \frac{1}{2}[(K_{11}^2 - K_{22}^2)^2 + 4K_{12}^2 K_{21}^2]^{1/2}$$

(when $i=1$ the + sign is taken, when $i=2$ the - sign is taken). The j 's are spherical Bessel functions and a_{11} and a_{22} are arbitrary constants.

Outside the range of nuclear forces ($r > R$) the potential is the Coulomb potential and the radial equations are uncoupled, with the usual (real) Coulomb functions F_l and G_l as solutions in each channel. The l subscript will be suppressed. Ingoing waves (u^-) and outgoing waves (u^+) are constructed:

$$u^\pm = e^{\mp i\omega} (F \pm iG), \quad (6)$$

where ω is the difference between the Coulomb phase shifts for the channel l value and $l=0$. If the incident beam is always taken to be in channel 1, the combination of u^\pm must be

$$u_1 \propto [-u_1^- + \alpha_1 e^{2i(\delta_1 + \omega_1)} u_1^+] \quad (7)$$

and in channel 2, where there are only outgoing waves

$$u_2 \propto \alpha_2 e^{2i(\delta_2 + \omega_2)} u_2^+. \quad (8)$$

If only one channel is open, $\alpha_1 = 1$ in Eq. (7), and Eq. (8) is modified to contain decaying exponential functions. A complex phase may then be removed from the expression in parentheses in Eq. (7) to leave the quantity inside real. Then a_{11} and a_{22} may be taken real, apart from the unimportant over-all complex phase. However, if both channels are open, $\alpha_1 < 1$ and a_{11} and a_{22} must be taken to be complex. Matching value and derivative for the complex radial wave functions in channels 1 and 2 gives four complex conditions on the four complex constants a_{11} , a_{22} , $\alpha_1 e^{2i(\delta_1 + \omega_1)}$, and $\alpha_2 e^{2i(\delta_2 + \omega_2)}$, where ω_1 and ω_2 are known.

FIG. 5. The solid curves are the phase shifts for an incident $l=0$ neutron wave in the elastic channel ($C^{12} + n$), the energies being indicated by the lower scale. As the coupling potential V_{12} is increased from top to bottom, a resonance "appears" in this channel. The dashed curves are the phase shifts for an incident wave in the inelastic channel ($C^{12*} + n$). The resonance "disappears" from this channel. The phase shift scale is in hundreds of degrees, but the curves are arbitrarily shifted relative to this scale.

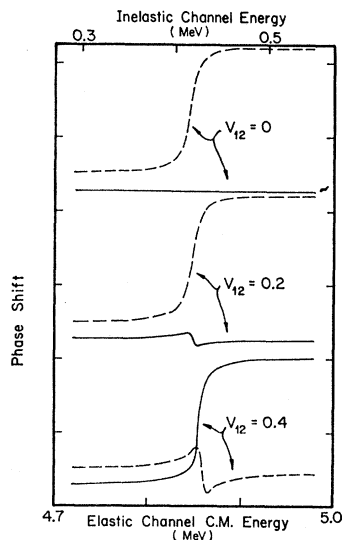
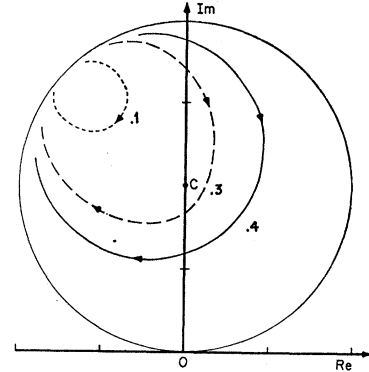


FIG. 6. The behavior of the scattering amplitude in the complex plane for an incident $l=0$ neutron wave in the elastic channel ($C^{12} + n$) as the energy is increased. The progression is in the direction of the arrow. The various curves are for different values of V_{12} , the values used appearing close to the curves.



Some sample results of the calculation will now be given, particularly concerning changes in the qualitative behavior of the phase shifts with energy as the coupling potential V_{12} is changed. Channel 1, which has the incident wave, is first taken to be ($C^{12} + n$), i.e., there is a neutron beam incident upon carbon-12 in its ground state. The l value is taken to be $l_1 = 0$. Channel 2 is first taken to be ($C^{12*} + n$) with $l_2 = 2$. The solid curves in Fig. 5 show the results as the coupling between the two channels is increased. With $V_{12} = 0$, $\alpha_1 = 1$ and the phase shift in the incident channel decreases monotonically with increasing neutron energy. Weak coupling ($V_{12} = 0.2$ MeV) produces an anomaly in the phase shift δ_1 , but it does not resonate, i.e., it does not pass through $\pi/2$. For stronger coupling ($V_{12} = 0.4$ MeV) as the neutron energy is increased δ_1 resonates.

Although it is not possible experimentally to use a C^{12*} target, it is simple to calculate for this case by having an $l=2$ incident beam in the inelastic channel. The phase shifts for this wave are shown as dashed curves in Fig. 5 for the three values of V_{12} . It can be seen that for $V_{12} = 0$ there is a resonance in this phase shift, but the resonance "disappears" at the same value of V_{12} for which it "appeared" in the phase shifts for an incident wave in the elastic channel. Thus the coupling moves the resonance from one channel to the other.

For the case of the incident wave in the elastic channel, the behavior of the scattering amplitude in the complex plane is shown in Fig. 6. It can be seen that the two types of behavior observed experimentally in the $d_{3/2}$ scattering amplitude (Fig. 4) occur for different coupling strengths.

III. FITS TO THE EXPERIMENTAL DATA

Throughout these calculations the nuclear force was represented by a square well of radius $R = 4.5 F$ and $l=0$ wave functions were used for $r < R$.

As a preliminary, single-channel calculations were made for s - and d -wave protons incident on C^{12} . In this s -wave case, choosing $V = -69.87$ MeV gave a resonance at $E_p = 0.464$ MeV with width $\Gamma = 36$ keV com-

pared to experimental values $E_p=0.461$ MeV, $\Gamma=34$ keV. The calculated phase shift is shown as a solid curve on Fig. 1. For the d -wave cases, $V=-71.00$ MeV gave a resonance at $E_p=1.740$ MeV, to correspond to the $d_{5/2}$ resonance at 1.748 MeV and $V=-64.25$ MeV gave a resonance at $E_p\approx 6.7$ MeV corresponding to the $d_{3/2}$ resonance in this energy region. Both d -wave calculated resonances were wider than those observed experimentally, since coupling to other channels, open and closed, was neglected.

Two-channel calculations were then made for energies above the inelastic threshold by setting the coupling potential V_{12} to a nonzero value. Since the number of channels in the calculation was limited to two, one of which was the elastic channel, it was necessary to assume that the inelastic channel was *either* $l=0$ or $l=2$. In practice both would be involved.

$d_{3/2}$ Phase Shifts

Channel 1 was taken to be $(C^{12}+p)$ with $l_1=2$ and channel 2 was first assumed to be $(C^{12*}+p)$ with $l_2=0$. The potentials V_{11} and V_{22} were fixed at -64.25 and -69.87 MeV respectively, the values determined by the single-channel calculations above. Thus the potential for $(C^{12*}+p)$ with $l=0$ was taken to be the same as that for $(C^{12}+p)$ with $l=0$. The calculated results for α_1 and δ_1 as a function of energy appear as dashed lines on Fig. 3. It can be seen that the calculated anomaly is about 120 keV below the experimentally observed location. In this calculation the only adjustable parameter was V_{12} , which was adjusted to fit the observed strength of the anomaly.

In the next calculation all three potentials V_{11} , V_{22} , and V_{12} were adjusted to give a good fit to the experimental data in the region of the 5.3-MeV anomaly. The calculated values of α_1 and δ_1 as a function of energy are shown as solid curves on Figs. 3 and 4. For ease of reference, the input quantities used for the calculation are listed in Table I. The potentials V_{11} and V_{22} were only slightly changed from their single-channel values, the changes being $+50$ and $+340$ keV, respectively. The coupling potential was $V_{12}=0.49$ MeV. It can be seen that the agreement is satisfactory over the 5.3-MeV anomaly, but deteriorates above

TABLE I. Parameter values used to calculate the $d_{3/2}$ curves in Figs. 3 and 4.

Channel 1:	Channel 2:
$C^{12}(p,p)C^{12}$	$C^{12}(p,p')C^{12*}$ ($Q=-4.43$ MeV)
	$R=4.5$ F
	$V_{11}=-64.20$ MeV
	$V_{22}=-69.53$ MeV
	$V_{12}=0.49$ MeV
	$l_1=2$
	$l_2=0$

about 6.5 MeV. This is believed due to the neglect of the $l=2$ inelastic channel in the calculation. The use of "square-well" potentials also presumably restricts the quality of the fits obtainable.

Calculations were also made with a slightly stronger coupling potential V_{12} and the results are shown as dashed curve on Fig. 4. The path of the scattering amplitude in this case includes C and passes up to the next Riemann sheet.

The calculations were repeated assuming that the $l=2$ inelastic channel was dominant at the 5.3-MeV anomaly. However the calculated anomaly in this case was much narrower than the experimental anomaly, and so it is believed that the $l=0$ channel is in fact dominant. This is as expected for low energies in the inelastic channel and is in agreement with the results of Bearse *et al.*,⁸ who were able to fit $C^{12}(p,p'\gamma)C^{12}$ angular correlation data at the 5.3-MeV anomaly assuming $l=0$ in the inelastic channel.

$d_{5/2}$ Phase Shifts

The single-channel value of the $l=0$ potential gave a resonance at 0.464 MeV in this channel. If V_{22} is chosen slightly more negative than this potential, the resonance in the inelastic channel will appear very close to threshold. Experimentally the resonance is found at $E_p=4.808$ MeV, compared to the threshold of approximately 4.800 MeV. Calculations were made with a potential for the inelastic channel of $V_{22}=-70.94$ MeV (i.e., deeper by 1.07 MeV than in the single-channel case) and the same coupling potential $V_{12}=0.49$ MeV that gave the best fit to the $d_{3/2}$ anomaly. The results for δ_1 as a function of energy are shown as a solid curve on Fig. 2. The input quantities used for the calculation are listed in Table II. A narrow resonance

TABLE II. Parameter values used to calculate the $d_{5/2}$ curve in Fig. 2.

Channel 1:	Channel 2:
$C^{12}(p,p)C^{12}$	$C^{12}(p,p')C^{12*}$ ($Q=-4.43$ MeV)
	$R=4.5$ F
	$V_{11}=-71.00$ MeV
	$V_{22}=-70.94$ MeV
	$V_{12}=0.49$ MeV
	$l_1=2$
	$l_2=0$

in the $d_{5/2}$ phase shift appears at an energy $E_p=4.807$ MeV and width $\Gamma\approx 8$ keV. The calculated damping parameter α_1 does not here deviate from unity, in contrast to its behavior over the 5.3-MeV $d_{3/2}$ anomaly. These calculated results for α_1 and δ_1 are in good agreement with the values found experimentally.

⁸ R. C. Bearse, J. C. Legg, G. C. Phillips, A. A. Rollefson, and G. Roy, Nucl. Phys. **65**, 545 (1965).

IV. CONCLUSIONS

The main features of the behavior of the $s_{1/2}$, $d_{3/2}$, and $d_{5/2}$ phase shifts and damping parameters for $C^{12}+p$ at $E_p \leq 6.5$ MeV have been explained by a coupled-channels calculation. The $d_{5/2}$ resonance at $E_p = 4.808$ MeV and the $d_{3/2}$ anomaly at $E_p \approx 5.3$ MeV have been shown to be caused by a low energy s -wave resonance in the ($C^{12}+p$) channel, closely corresponding to the 0.461-MeV $s_{1/2}$ resonance in the elastic channel. The diagonal parts of the potentials used have the following relation:

$$|V(d_{5/2})| > |V(s_{1/2})| > |V(d_{3/2})|.$$

This relation is consistent with the existence of a spin-orbit interaction with the usual sign.

ACKNOWLEDGMENTS

The author is extremely grateful to Professor T. A. Tombrello for the encouragement, help and advice he has given on many occasions. Dr. W. P. Timlake gave substantial help on the mathematical aspects of this problem and Professor Ian Duck and Professor E. B. Paul contributed through several enlightening discussions.

Theory of Pion Absorption Applied to the Reaction $Li^6(\pi^-, 2n)He^4$ †

D. S. KOLTUN

Department of Physics and Astronomy, University of Rochester, Rochester, New York

AND

A. REITAN*

Department of Physics and Astronomy, University of Rochester, Rochester, New York
and*Norges Tekniske Høgskole, Trondheim, Norway*

(Received 3 October 1966)

The absorption of pions from a low-energy S state, by a nucleus with the emission of two fast nucleons, is treated in an impulse approximation in which the pion interacts only with the pair of ejected nucleons. We consider the particular reaction $Li^6(\pi^-, 2n)He^4$. The two-nucleon absorption process is given by a theory, previously applied to the pion absorption by a deuteron, which is developed from low-energy pion-nucleon scattering theory. The relative motion of the absorbing nucleon pair is treated in detail, including effects of short-range repulsion and tensor potentials. Distributions of the emitted nucleons in momentum and angle are calculated in this theory, and are compared with other results for some theories and with experimental data.

I. INTRODUCTION

THE reaction in which a nucleus absorbs a slow pion and emits two fast nucleons has been attractive for theoretical consideration since kinematical conditions seem favorable to some form of impulse approximation. The notion is that two colliding nucleons in a nucleus may convert the rest energy of the pion to kinetic energy with little transfer of momentum to the residual nucleus. If the probability is high that these two nucleons will escape with little further interaction with the residual nucleus, it is inviting to try to treat the problem in two parts: the absorption of a pion by two nucleons, and the motion of the two nucleons in a nucleus. This approach was first introduced in the work of Brueckner, Serber, and

Watson¹ who attempted to relate the rate for pion absorption in nuclei to the absorption of a pion by a free deuteron.

More recently a model along these lines has been applied to the absorption of S -wave pions by various light nuclei, by Eckstein² for He^4 , by Divakaran³ for He^3 , by Sakamoto⁴ for Li^6 , and by M. Ericson⁵ for several cases. These calculations have in common a model interaction which includes both the pion interaction with a nucleon pair, and the short-range correlation of the nucleon pair in its initial state. The strength parameters of the assumed interaction are fixed to give the experimental cross sections for thresh-

¹ K. Brueckner, R. Serber, and K. Watson, Phys. Rev. **84**, 258 (1951).

² S. G. Eckstein, Phys. Rev. **129**, B387 (1963).

³ P. P. Divakaran, Phys. Rev. **139**, B387 (1965).

⁴ Y. Sakamoto, Nuovo Cimento **37**, 775 (1965).

⁵ M. Ericson, Compt. Rend. **258**, 1471 (1964).

† Work supported in part by the U. S. Atomic Energy Commission.

* Permanent address: Norges Tekniske Høgskole, Trondheim, Norway.